LETTERS

Stoichiometry and turnover in single, functioning membrane protein complexes

Mark C. Leake[1]*, Jennifer H. Chandler[2]*, George H. Wadhams[2], Fan Bai[1], Richard M. Berry[1] & Judith P. Armitage[2]

Many essential cellular processes are carried out by complex biological machines located in the cell membrane. The bacterial flagellar motor is a large membrane-spanning protein complex that functions as an ion-driven rotary motor to propel cells through liquid media[1–3]. Within the motor, MotB is a component of the stator that couples ion flow to torque generation and anchors the stator to the cell wall[4,5]. Here we have investigated the protein stoichiometry, dynamics and turnover of MotB with single-molecule precision in functioning bacterial flagellar motors in *Escherichia coli*. We monitored motor function by rotation of a tethered cell body[6], and simultaneously measured the number and dynamics of MotB molecules labelled with green fluorescent protein (GFP–MotB) in the motor by total internal reflection fluorescence microscopy. Counting fluorophores by the stepwise photobleaching of single GFP molecules showed that each motor contains ~22 copies of GFP–MotB, consistent with ~11 stators each containing two MotB molecules. We also observed a membrane pool of ~200 GFP–MotB molecules diffusing at ~0.008 $\mu m^2 s^{-1}$. Fluorescence recovery after photobleaching and fluorescence loss in photobleaching showed turnover of GFP–MotB between the membrane pool and motor with a rate constant of the order of 0.04 s^{-1}: the dwell time of a given stator in the motor is only ~0.5 min. This is the first direct measurement of the number and rapid turnover of protein subunits within a functioning molecular machine.

Over 30% of all proteins are integrated in biological membranes, where they carry out diverse essential cellular functions. Many membrane proteins function in multimeric complexes, and investigating their organization and dynamics is essential for understanding their function. GFP fusion constructs[7] have been used with total internal reflection fluorescence (TIRF) microscopy to detect single interactions at the basal membrane *in vivo*[8], and fluorescence recovery after photobleaching (FRAP) and fluorescence loss in photobleaching (FLIP) have been used to measure dynamics of membrane protein populations[9–12]. Little is understood, however, about protein dynamics and turnover within individual complexes under natural conditions in living cells. Here we show that protein components of a functioning biological machine undergo rapid exchange with a freely diffusing pool in the cell membrane.

The bacterial flagellar motor is ideal for examining a single protein complex *in vivo*; rotation of the whole cell when the filament is attached to a surface (Fig. 1) is an instantaneous indicator of motor function. Previous research indicates that a motor has 8–16 stators[4,5,13–15], each containing two copies of MotB and four copies of MotA[16]. We replaced genomic *motB* in *E. coli* with *gfp–motB* to express GFP–MotB in wild-type amounts (see Methods). Polystyrene beads (0.75 μm in diameter) attached to filaments[17] rotated three times slower than on the parental strain (Supplementary Fig. 3), indicating some reduction in GFP–MotB function. We attached live cells to a coverslip either by the filament ('tethered') or by the cell body ('stuck') and observed them with TIRF or brightfield microscopy (Fig. 1a). TIRF images of tethered cells showed spots at the centre of cell rotation measured from brightfield images (Fig. 1c, Supplementary Videos 1 and 2). Similar spots were observed for stuck cells, with one or occasionally two spots visible. Spot size and

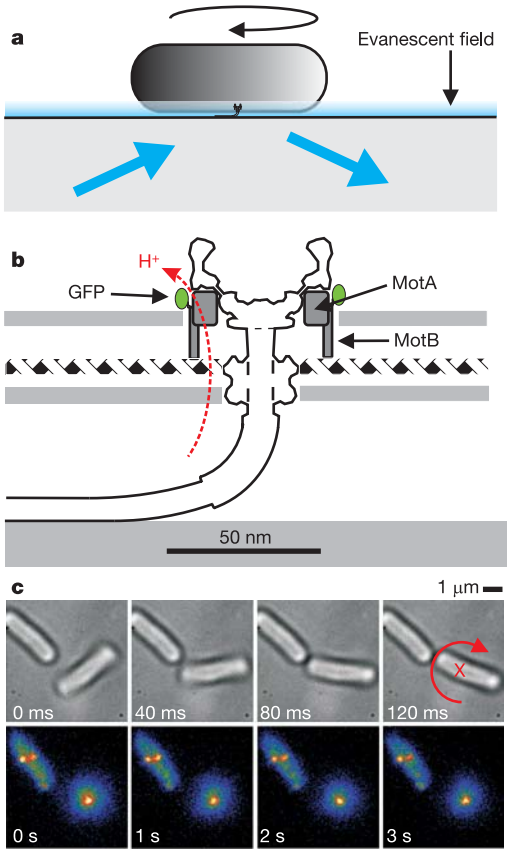

Figure 1 | TIRF microscopy of live GFP–MotB cells. a, **b**, Antibody-tethered cell rotation assay (**a**) and expansion of the motor structure (**b**). Coverslip and cell membranes are light grey, the cell wall is hatched, and TIRF illumination is blue-green. **c**, Consecutive brightfield (top) and TIRF (bottom) images showing a rotating tethered GFP–MotB cell and a nearby stuck cell. Rotation of the freely tethered cell is indicated in red. Two motor spots are visible in the stuck cell, whereas one is visible at the centre of rotation in the tethered cell.

[1]Clarendon Laboratory, Department of Physics, University of Oxford, Parks Road, Oxford OX1 3PU, UK. [2]Microbiology Unit, Department of Biochemistry, University of Oxford, South Parks Road, Oxford OX1 3QU, UK.
*These authors contributed equally to this work.

Table 1 | Photobleach parameters for different cellular components

Component*	Initial intensity (I_0)	Time constant (t_0)
Motor GFP–MotB	103,000 ± 3,300 counts s^{-1}	44 ± 1 s
Membrane GFP–MotB	280 ± 50 counts s^{-1} $pixel^{-1}$	269 ± 8 s
Cell autofluorescence	1,351 ± 42 counts s^{-1} $pixel^{-1}$	62 ± 1 s

*Data are from 134 ROIs in GFP–MotB cells containing motors (row 1), 27 ROIs in GFP–MotB cells containing no motors (row 2), and 32 ROIs in cells lacking GFP–MotB (row 3). Data are mean ± s.e.m.

number were consistent with a ring of GFP–MotB molecules bordering a rotor with a diameter of ~50 nm (refs 14, 18; Fig. 1b) and ~6 motors per cell[19] (Supplementary Note 1).

We modelled fluorescence intensity (I) in 400-nm square regions of interest (ROIs) containing a single motor as a uniform background plus a gaussian spot of width 300 nm (motor width plus microscope point-spread function) and identified three background components: GFP–MotB in the membrane, nonspecific cellular autofluorescence and instrumental background (Supplementary Methods 2). Cytoplasmic GFP and autofluorescence were not expected to contribute because only the cell surface adjacent to the coverslip was illuminated. We estimated instrumental background from an empty ROI close to the cell in each image and autofluorescence from the parental strain. All cellular components showed roughly exponential photobleaching under TIRF illumination: $I(t) = I_0 exp(-t/t_0)$ (Fig. 2a, Table 1 and Supplementary Fig. 4). The GFP membrane component bleached considerably more slowly than the motor, which we attribute to diffusive exchange with unbleached fluorophores from outside the TIRF field.

Total intensity (minus instrumental background) in ROIs containing motors photobleached in steps at roughly integer multiples of a unitary level, I_{GFP}, consistent with photobleaching of individual GFP molecules[20,21] (Fig. 2b, e). Separation into motor and background components introduced extra noise (Fig. 2a); therefore, we calculated I_{GFP} using total intensity rather than the motor component alone. Figure 2c and d shows the pairwise-distance distribution function (PDDF; Supplementary Methods 3) and its power spectrum, respectively, for the filtered curve 3 in Fig. 2b (refs 22, 23). The peak in the power spectrum indicates a unitary step size of $I_{GFP} \approx 5{,}400$ counts (ref. 23). To confirm that this corresponds to bleaching of one GFP molecule, we reduced the background fluorescence by prebleaching the cell, facilitating direct observation of successive photobleaching steps in the motor component of fluorescence (Fig. 2e and Supplementary Methods 4). The double-sized step in Fig. 2e presumably corresponds to two successive unitary photobleaches that were not resolved by the filtering algorithm; furthermore, no steps were detected in photobleaches of the parental strain. Step-wise photobleaching of single surface-immobilized GFP molecules[24] showed an average step size of ~13,000 counts s^{-1} in our microscope, after correcting for differences in laser power and exposure time (Fig. 2f). TIRF intensity falls exponentially with distance over ~100 nm (Supplementary Methods 5); thus, the average value of I_{GFP} is consistent with motors being ~90 nm from the coverslip.

Supplementary Fig. 5a and b show distributions of I_{GFP} and initial motor intensities (I_0^m), respectively, for 134 traces from different cells. The widths probably reflect different TIRF intensities, which varied about fourfold over the measured range of cell heights (~150 nm) owing to different distances from motor to coverslip. We estimated the total number of GFP–MotB molecules per motor by dividing I_0^m by I_{GFP} for each trace (Supplementary Fig. 5c). The reduced uncertainty of this estimate (22 ± 6, ±s.d.) as compared with the ratio of peaks in Supplementary Fig. 5a and b (19 ± 8) reflects covariation of I_0^m and I_{GFP}, as expected for variations due to TIRF intensity. Dividing the initial membrane component of

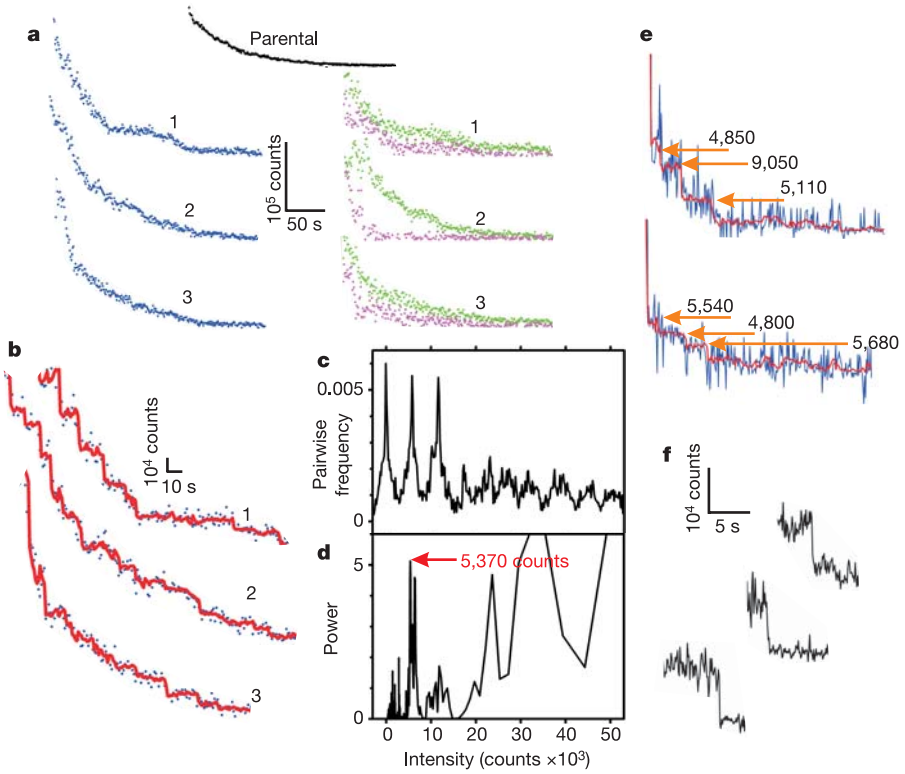

Figure 2 | TIRF photobleaching. **a**, Three photobleaches for regions centred on motors, showing total (blue), motor (magenta) and background (green) intensities, and average autofluorescence (black) from 32 parental cells lacking GFP. **b**, Expansions from traces in **a** with C–K-filtered traces overlaid (red). **c**, **d**, PDDF (**c**) and power spectrum of the PDDF (**d**) for filtered intensity curve 3 in **a**; the unitary peak is indicated (arrow). **e**, Stepwise photobleaching of motors after prebleaching of the cell to reduce background. The motor component (blue), C–K-filtered trace (red), steps detected and step sizes are indicated (arrows). **f**, Stepwise photobleaching of surface-immobilized GFP molecules[24].

background intensity by I_{GFP} gave an average of 0.052 ± 0.022 molecules per pixel. We estimated the cell-surface area as 3,700 ± 500 pixels; thus, the total number of non-motor GFP–MotB molecules per cell is 190 ± 80.

We investigated protein turnover between membrane and motor components using focused laser exposures of 0.5 s to photobleach all fluorophores in regions with a width of ~1 μm. Figure 3a shows TIRF images of a cell before and after bleaching of a region containing a motor. Fluorescence recovery (FRAP) of both motor and background components in the bleached region is visible, as is fluorescence loss ('one-shot' FLIP; Supplementary Methods 5) at the other end of the cell. FRAP and FLIP (Fig. 3b) of motor and membrane components respectively, averaged over 13–38 cells, are shown in Fig. 3c and d. Both components recovered over the course of a few minutes; motor recovery was slightly delayed as compared with membrane. Fluorescence loss occurred on the same timescale in both components.

Fitting all of the membrane FRAP data from ROIs lacking motors to a model of a diffusing GFP–MotB membrane pool gave a diffusion coefficient, D, of 0.0075 ± 0.0013 $\mu m^2 s^{-1}$ (Supplementary Methods 6). We obtained an independent, single-molecule estimate, $D = 0.0088 \pm 0.0026\ \mu m^2 s^{-1}$, by tracking mobile fluorescent spots

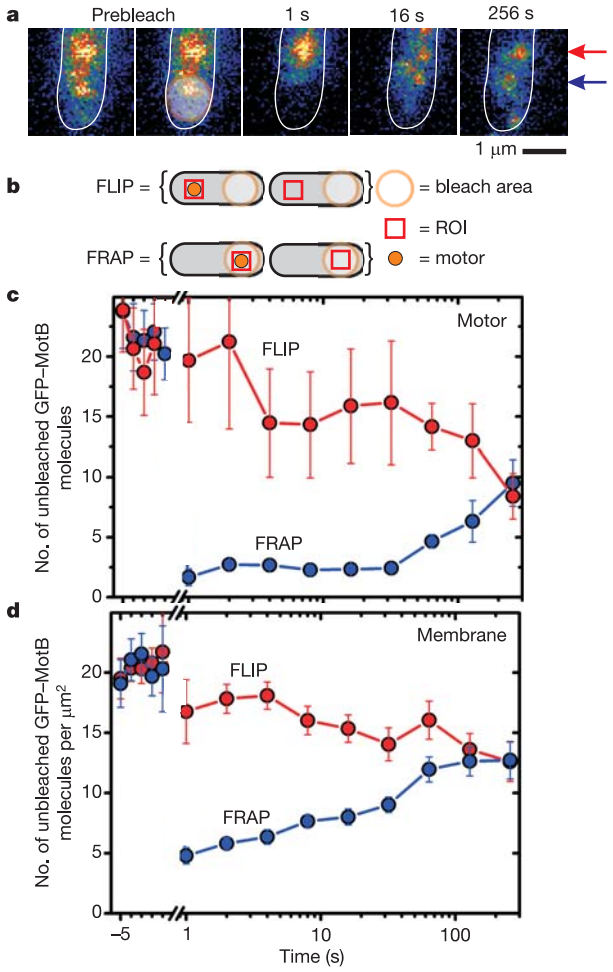

Figure 3 | Focused laser FRAP and 'one-shot' FLIP. a, Successive TIRF images of a GFP–MotB cell before and after bleaching. The prebleach images are identical; the laser focus is indicated (circle, right panel). Arrows indicate positions of two motors, showing FLIP (red) and FRAP (blue); the cell is outlined (white). **b**, Representation of FLIP and FRAP using ROIs with and without motors. **c**, **d**, Mean numbers of unbleached GFP–MotB molecules in motor (**c**) and membrane (**d**) components versus time. Data points were an average of 13 (motor, FLIP), 30 (motor, FRAP) and 38 (membrane) ROIs. Errors bars indicate 1 s.d.

that could occasionally be resolved after prebleaching (Supplementary Methods 6 and Supplementary Videos 3 and 4). The intensity of these spots was consistent with a GFP–MotB dimer (Supplementary Fig. 9). Fitting all of the FRAP and FLIP data to an extended diffusion model, incorporating binding and unbinding at the motor and bleaching in the TIRF field (Supplementary Methods 7), gave a dissociation rate at the motor of 0.04 ± 0.02 s^{-1}. The large uncertainty is a consequence of the small difference between recovery rates of motor and membrane components relative to noise. We also studied slow recovery after complete bleaching of whole cells (Supplementary Methods 8 and Supplementary Videos 5–7). After 90 min, fluorescence recovery ranged from 75% in buffer enriched with nutrients to 7% with protein synthesis blocked (attributable to GFP maturation[7]).

Fluorophore counting indicated that there are 22 ± 6 GFP–MotB molecules per motor. We confirmed the accuracy of the counting by testing it against simulated TIRF photobleach traces generated by the extended diffusion model (Supplementary Fig. 11). We also measured very low fluorescence anisotropy in motors after bleaching with polarized light (Supplementary Methods 9), indicating that GFP fluorophores in motors are free to rotate and therefore all are counted by the photobleaching method. Measurements of solubility and copurification with MotA suggest that MotB is stable in the cytoplasmic membrane only as a dimer in 1:2 stoichiometry with MotA[16]. This suggests that, on average, a motor has 11 stators, each with the composition $MotA_4$:$MotB_2$. Early work estimated 16 stators in a motor[4], whereas subsequent studies estimated 8 stators[5]. We previously observed at least 11 discrete speed increments after induced expression of functional Mot proteins in a defective background[15]. Our photobleaching result also agrees with freeze-fracture electron microscopy showing 11–12 stators around the rotor[14]. The broad distributions in our counting estimates may include both natural variation in the number of stators per motor and noise due to background fluorescence, GFP blinking[20] and instrumental limitations. We measured a mobile membrane pool of ~200 GFP–MotB molecules with $D \approx 0.008\ \mu m^2 s^{-1}$, which is ~40% smaller than the diffusion rate measured for free membrane proteins of comparable size to a GFP–MotB dimer[25], and only ~20% smaller than that for a $MotA_4$:$(GFP–MotB)_2$ stator, assuming that the Stokes radius r scales to the 1/3 power with molecular weight and that D scales as $1/r$. A relatively high value of D agrees with other data suggesting that MotB in the membrane pool does not bind significantly to the cell wall[26]. Eleven stators, each with a dissociation rate ~0.04 s^{-1}, gives an overall exchange of ~0.44 stators per s.

In summary, by replacing wild-type *motB* in the genome with *gfp–motB*, we expressed the fusion protein in natural quantities, enabling us to investigate protein stoichiometry and dynamics under physiological conditions. Our methods for counting the number of proteins in a membrane complex in living cells and observing their turnover using TIRF microscopy should be applicable to other membrane protein complexes. Unexpectedly, an anchored component, MotB[27], of a multiprotein complex was found to diffuse in the membrane and exchange rapidly with the motor, a finding that may alter the conventional 'static' view of molecular complexes; if proteins in the flagellar motor are undergoing dynamic exchange, this finding may well apply to other macromolecular complexes. It should be possible using similar methods to learn whether other membrane proteins also turnover rapidly and, if not, to investigate possible reasons for differences between complexes.

METHODS

***E. coli* strains and cell preparation.** A strain expressing GFP–MotB from the genome in normal MotB physiological quantities was constructed, and cells were prepared as described in Supplementary Methods 1.

Fluorescence microscopy. We used a home-built inverted TIRF microscope with an excitation wavelength of 488 nm (Supplementary Methods 5). Fluorescence emission was imaged at ~50 nm per pixel in frame-transfer mode at 1 Hz

(25 Hz for immobilized GFP molecules, 10 Hz for particle tracking) by a 128 × 128-pixel, cooled, back-thinned electron-multiplying charge-coupled-device camera (iXon DV860-BI, Andor Technology).

Image acquisition and photobleaching. Images were sampled continuously for 300 s, resulting in >90% photobleaching within range of the TIRF field. For FRAP and FLIP experiments, single TIRF exposures were taken at intervals up to 256 s after bleaching with a focused laser spot for 0.5 s, centred either over a fluorescent spot of a putative motor (FRAP) or >1 μm from a motor (FLIP). Motor and membrane components were separated as described in the text for TIRF bleaches. Average curves were generated for FRAP and FLIP of both motor and membrane components; all intensity components were corrected for photobleaching (Supplementary Methods 5).

Data analysis and simulations. Continuous TIRF intensity data were filtered by using a Chung–Kennedy (C–K) algorithm[22]; spatial frequency analysis of the pairwise intensity-difference histograms was used to determine the unitary step size[23]; membrane diffusion was modelled by using Monte Carlo simulations for mobility of single GFP–MotB molecules; rate constants for the turnover process at the motor were evaluated by using a least-squares fit to FRAP and FLIP data (see Supplementary Information for details).

Received 21 June; accepted 24 July 2006.
Published online 13 September 2006.

1. Macnab, R. M. in *Escherichia coli and Salmonella: Cellular and Molecular Biology* (ed. Neidhardt, F. C.) 123–145 (American Society for Microbiology, Washington DC, 1996).
2. Berry, R. M. & Armitage, J. P. The bacterial flagella motor. *Adv. Microb. Physiol.* **41,** 291–337 (1999).
3. Berg, H. C. The rotary motor of bacterial flagella. *Annu. Rev. Biochem.* **72,** 19–54 (2003).
4. Block, S. M. & Berg, H. C. Successive incorporation of force-generating units in the bacterial rotary motor. *Nature* **309,** 470–472 (1984).
5. Blair, D. F. & Berg, H. C. Restoration of torque in defective flagellar motors. *Science* **242,** 1678–1681 (1988).
6. Silverman, M. & Simon, M. Flagellar rotation and the mechanism of bacterial motility. *Nature* **249,** 73–74 (1974).
7. Tsien, R. Y. The green fluorescent protein. *Annu. Rev. Biochem.* **67,** 509–544 (1998).
8. Mashanov, G. I., Tacon, D., Peckham, M. & Molloy, J. E. The spatial and temporal dynamics of pleckstrin homology domain binding at the plasma membrane measured by imaging single molecules in live mouse myoblasts. *J. Biol. Chem.* **279,** 15274–15280 (2004).
9. Mullineaux, C. W. & Sarcina, M. Probing the dynamics of photosynthetic membranes with fluorescence recovery after photobleaching. *Trends Plant Sci.* **7,** 237–240 (2002).
10. Ray, N., Nenninger, A., Mullineaux, C. W. & Robinson, C. Location and mobility of twin-arginine translocase subunits in the *Escherichia coli* plasma membrane. *J. Biol. Chem.* **280,** 17961–17968 (2005).
11. Goodwin, J. S. & Kenworthy, A. K. Photobleaching approaches to investigate diffusional mobility and trafficking of Ras in living cells. *Methods* **37,** 154–164 (2005).
12. Mullineaux, C. W., Nenninger, A., Ray, N. & Robinson, C. Diffusion of green fluorescent protein in three cell environments in *Escherichia coli*. *J. Bacteriol.* **188,** 3442–3448 (2006).
13. Berry, R. M., Turner, L. & Berg, H. C. Mechanical limits of bacterial flagellar motors probed by electrorotation. *Biophys. J.* **69,** 280–286 (1995).
14. Khan, S., Dapice, M. & Reese, T. S. Effects of *mot* gene expression on the structure of the flagellar motor. *J. Mol. Biol.* **202,** 575–584 (1988).
15. Reid, S. W. *et al.* The maximum number of torque-generating units in the flagellar motor of *Escherichia coli* is at least 11. *Proc. Natl Acad. Sci. USA* **103,** 8066–8071 (2006).
16. Kojima, S. & Blair, D. F. Solubilization and purification of the MotA/MotB complex of *Escherichia coli*. *Biochemistry* **43,** 26–34 (2004).
17. Sowa, Y. *et al.* Direct observation of steps in rotation of the bacterial flagellar motor. *Nature* **437,** 916–919 (2005).
18. Sourjik, V. & Berg, H. C. Localization of components of the chemotaxis machinery of *Escherichia coli* using fluorescent protein fusions. *Mol. Microbiol.* **37,** 740–751 (2000).
19. Turner, L., Ryu, W. S. & Berg, H. C. Real-time imaging of fluorescent flagellar filaments. *J. Bacteriol.* **182,** 2793–2801 (2000).
20. Dickson, R. M., Cubitt, A. B., Tsien, R. Y. & Moerner, W. E. On/off blinking and switching behaviour of single molecules of green fluorescent protein. *Nature* **388,** 355–358 (1997).
21. Chu, S. Biology and polymer physics at the single-molecule level. *Phil. Trans. R. Soc. Lond. A* **361,** 689–698 (2003).
22. Leake, M. C., Wilson, D., Gautel, M. & Simmons, R. M. The elasticity of single titin molecules using a two-bead optical tweezers assay. *Biophys. J.* **87,** 1112–1135 (2004).
23. Svoboda, K., Schmidt, C. F., Schnapp, B. J. & Block, S. M. Direct observation of kinesin stepping by optical trapping interferometry. *Nature* **365,** 721–727 (1993).
24. Mashanov, G. I., Tacon, D., Knight, A. E., Peckham, M. & Molloy, J. E. Visualizing single molecules inside living cells using total internal reflection fluorescence microscopy. *Methods* **29,** 142–152 (2003).
25. Deich, J., Judd, E. M., McAdams, H. H. & Moerner, W. E. Visualization of the movement of single histidine kinase molecules in live Caulobacter cells. *Proc. Natl Acad. Sci. USA* **101,** 15921–15926 (2004).
26. Van Way, S. M., Hosking, E. R., Braun, T. F. & Manson, M. D. Mot protein assembly into the bacterial flagellum: a model based on mutational analysis of the *motB* gene. *J. Mol. Biol.* **297,** 7–24 (2000).
27. Demot, R. & Vanderleyden, J. The C-terminal sequence conservation between OMPA-related outer membrane proteins and MotB suggests a common function in both gram-positive and gram-negative bacteria, possibly in the interaction of these domains peptidoglycan. *Mol. Microbiol.* **12,** 333–336 (1994).

Supplementary Information is linked to the online version of the paper at www.nature.com/nature.

Acknowledgements We thank D. Blair for antibodies to flagellin and MotB. The research of M.C.L., J.H.C., R.M.B. and J.P.A. was supported by combined UK research councils via an Interdisciplinary Research Collaboration in Bionanotechnology (IRC), that of G.H.W. by the Biotechnology and Biological Sciences Research Council (BBSRC), and that of F.B. by a Clarendon Scholarship.

Author Contributions Fluorescence experiments were carried out by M.C.L. and J.H.C. in the laboratory of R.M.B.; strain construction was done by J.H.C. and G.H.W. in the laboratory of J.P.A.; data analysis was done by M.C.L., R.M.B. and G.H.W.; and simulations were carried out by F.B. and M.C.L. The experiment was designed by M.C.L., R.M.B. and J.P.A.

Author Information Reprints and permissions information is available at www.nature.com/reprints. The authors declare no competing financial interests. Correspondence and requests for materials should be addressed to J.P.A. (judith.armitage@bioch.ox.ac.uk).